Styrene polymerized in an oil-in-water microemulsion

Hsiang-In Tang, Patricia L. Johnson and Esin Gulari
Department of Chemical and Metallurgical Engineering, Wayne State University, Detroit, Michigan 48202, USA
(Received 26 September 1983)

Microemulsions of styrene dispersed in water using sodium dodecyl sulphate and pentanol and polystyrene, isolated after the polymerizations were carried out to completion, were studied by photon correlation spectroscopy and time-averaged intensity measurements. Microemulsions contained droplets 40.8 nm in diameter. It was found that the size distributions of polystyrene were bimodal. The results indicate that smaller droplets in a microemulsion provide an increased surface area which can complete with micelles in the capture of radicals. The bimodal nature of the products is evidence for two mechanisms of initiation and particle growth.

(Keywords: styrene polymerization; oil-in-water microemulsions; light scattering; polymerization)

INTRODUCTION

Microemulsions are thermodynamically stable colloidal dispersions of water in an organic medium, water-in-oil (W/O) type, or an organic medium in water, oil-in-water (O/W) type. They have been shown to be transparent systems with the dispersed phase consisting of droplets 5–100 nm in diameter[1]. Microemulsions provide suitable media for polymerization because by introducing the monomer in either the dispersed or the continuous phase, the outcome of a polymerization process can be altered. In a few recently reported studies, polymerizations have been achieved in microemulsions. Stoffer and Bone have polymerized methyl methacrylate[2] and methyl acrylate[3] in the continuous phase of W/O microemulsions. Leong and Candau[4] have prepared polyacrylamide by photo-polymerization in a W/O microemulsion where a water–acrylamide mixture was dispersed in toluene.

In this study microemulsions formed by styrene, water, sodium dodecyl sulphate (SDS), and pentanol were initiated by potassium persulphate. The polymerizations were carried out to completion. The microemulsions and the isolated polystyrene were studied by quasielastic light scattering techniques including both time-averaged intensity measurements and photon correlation spectroscopy (p.c.s.) to determine the average molecular weight and the polydispersity of these samples and thus provide explanation to mechanisms of polymerizations in O/W microemulsions with the monomer in the dispersed phase and the free-radical initiator soluble in the continuous phase.

EXPERIMENTAL

The reagents used were of the following purities. Styrene from Matheson Coleman and Bell Chemical, Inc. of 98% purity was further purified by vacuum distillation to remove the inhibitor. Pentanol was from Fisher Scientific Company of boiling range 137.2–138.0°C. Sodium dodecyl sulphate from Bio-Rad. Laboratories was of 99% electrophoresis purity reagent and was used without further purification.

The microemulsions were prepared by titrating various styrene, SDS, and pentanol mixtures with water containing initiator dissolved in it. In *Figure 1* microemulsion regions at 50°C are shown on a triangular plane, intersecting the SDS–pentanol–styrene plane at 27.3 wt.% styrene and extending to the apex representing pure water. The boundaries of the micro-emulsion regions were obtained by titrating with water various SDS–pentanol–styrene mixtures to the point of dissolution of SDS, determining the right-hand limit of the solubility region and then the clouding point defining

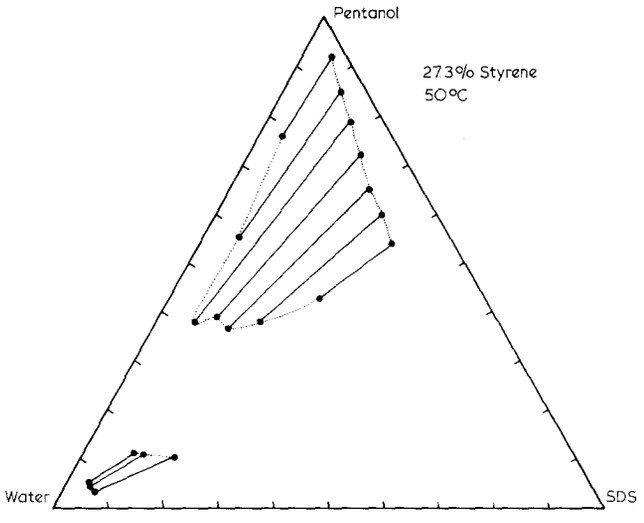

Figure 1 Microemulsion regions containing 27.3 wt.% styrene based on (SDS + pentanol + styrene) at 50°C

0032-3861/84/091357-06$03.00

the left-hand limit. There are two regions of solubility. The larger region, W/O region, corresponds to dispersion of water, ranging from 10 to 50 wt.% water, in a continuous phase containing styrene and pentanol. In the smaller region, O/W region, droplets containing styrene are dispersed in water ranging from 80 to 90 wt.%. The compositions of the microemulsions studies are listed in *Table 1* with the sample numbers identifying the type of microemulsion and the temperature at which polymerizations were carried out. Essentially, the three compositions are identical on a water-free basis, and correspond to compositions along a water dilution line in the O/W region. Ampules filled with the microemulsions were sealed under nitrogen and kept in a constant temperature bath at 50°C for eight days.

The polystyrene samples were isolated by standard procedures of filtration and washing with water and methanol followed by dissolving them in benzene and precipitating into methanol. For the light scattering measurements, the samples were dissolved in cyclohexane as follows: first, dry polystyrene was dissolved in benzene at room temperature and solutions at the desired concentrations were individually filtered (Millipore type GS, size 0.22 μm) directly into cells up to a marked volume. Then the benzene was evaporated and cyclohexane was added to the marked volume and the samples were stirred and conditioned at 38°C for several days.

The components of the light-scattering spectrometer were essentially similar to those described elsewhere[5]. We used a Spectra–Physics model 165 argon-ion laser operating at about 300 mW with $\lambda_0 = 514.5$ nm. The time-averaged intensity measurements were counted on a Hewlett-Packard Model 5316A universal counter. The correlation functions were computed by a Malvern Scientific Model K7025 real-time multibit correlator. The reference intensity was monitored by using a power meter coupled to a digital voltmeter. The photometer was controlled by a Hewlett-Packard Model 85 calculator.

METHODS OF DATA ANALYSIS

Intensity data

The Rayleigh ratio R_v for vertically polarized light at finite concentrations has the approximate form[6]

$$\frac{HC}{R_v} = \left(\frac{1}{M_w} + 2A_2C\right)\left[1 + (1+2A_2CM_w)^{-1}\frac{16\pi^2 n_0^2}{3\lambda_0^2} \times \langle r_g^2(C)\rangle_z \times \sin^2\frac{\theta}{2}\right] \quad (1)$$

where $H = 4\pi^2 n_0^2 (\partial n/\partial C)^2 / N_A \lambda_0^4$, with n_0, C, N_A, and λ_0 as, respectively, the refractive index, concentration, Avogadro's number, and wavelength of light *in vacuo* and $R_v = r^2 i_v / I_{ref}$, with r, i_v, and I_{ref} as the distance between the scattering centre and the point of observation, the excess vertically polarized scattered intensity, and the reference incident intensity, respectively. A plot of HC/R_v *versus* $\sin^2(\theta/2)$ yields the radius of gyration,

$$\langle r_g^2(C)_z^* = \frac{\langle r_g^2(C)\rangle_z}{1+2A_2CM_w} = \frac{\text{initial slope}}{\text{intercept}}\frac{3\lambda_0^2}{16\pi^2 n_0^2} \quad (2)$$

where $\langle r_g^2(C)\rangle_z [= \sum_i M_i C_i (r_g^2)_i / \sum_i M_i C_i]$ at infinite dilution is the square of radius of gyration. The terms A_2, and M_w are determined from a plot of $\lim_{\theta \to 0}(HC/R_v)$ *versus* C, where

$$\lim_{\theta \to 0}\frac{HC}{R_v} = \frac{1}{M_w} + 2A_2C \quad (3)$$

Correlation function data

The measured homodyne, intensity autocorrelation function has the form

$$G^{(2)}(I\Delta\tau) = A(1 + \beta|g^{(1)}(I\Delta\tau)|^2), \quad (4)$$

where $|g^{(1)}(\tau)|$ is the normalized correlation function of the scattered electric field; A, β, I, and $\Delta\tau$ are, respectively, the background, an adjustable parameter in the fitting procedure, the delay channel number, and the delay time increment; and $\tau = I\Delta\tau$. In the cumulants method[7],

$$\ln(A\beta)^{1/2}|g^{(1)}(\tau)| = \ln(A\beta)^{1/2} - \bar{\Gamma}\tau + \frac{1}{2!}\mu_2\tau^2 - \frac{1}{3!}\mu_3\tau^3 + \cdots \quad (5)$$

where

$$\bar{\Gamma} = \int_{\Gamma=0}^{\infty} \Gamma G(\Gamma)\,d\Gamma \quad (6)$$

and

$$\mu_i = \int_{\Gamma=0}^{\infty} (\Gamma - \bar{\Gamma})^i G(\Gamma)\,d\Gamma \quad (7)$$

where $G(\Gamma)$ is the normalized distribution of decay rates. For $Kr_g < 1$

$$\langle D\rangle_z = \frac{\sum C_i M_i D_i}{\sum C_i M_i} = \frac{\Gamma}{K^2} \quad (8)$$

where $K[\equiv 4\pi n_0/\lambda_0)\sin(\theta/2)]$ is the magnitude of the momentum transfer vector. At infinite dilution.

$$\langle D\rangle_z^0 = \frac{K_B T}{6\pi\eta\langle r_h\rangle} \quad (9)$$

where $\langle r_h\rangle [= \lim_{C\to 0}\sum_i C_i M_i / \sum_i (C_i M_i / r_{h,i})]$ is the weighted equivalent hydrodynamic radius η is the solvent viscosity.

In the histogram method[8], a discrete step function (a histogram) is used to approximate $G(\Gamma)$, such that

$$\sum_{j=1}^{n} G(\Gamma_i)\Delta\Gamma = 1 \quad (10)$$

and

$$|g^{(1)}(\tau)| = \sum_{j=1}^{n} G(\Gamma_j) \int_{\Gamma_j - \Delta\Gamma/2}^{\Gamma_j + \Gamma/2} \exp[-\Gamma I\Delta\tau)\,d\Gamma \quad (11)$$

where $G(\Gamma_j)$ represents the weighting factor based on integrated scattered intensity of molecules having line-

Table 1 Composition of O/W microemulsions

Component/ sample no.	Water (wt.%)	Styrene (wt.%)	SDS (wt.%)	Pentanol (wt.%)
O/W 50 I	86.9	3.56	6.11	3.39
O/W 50 II	77.1	6.24	10.69	5.94
O/W 50 III	83.3	4.56	7.80	4.34

widths from $\Gamma_j - \Delta\Gamma/2$ to $\Gamma_j + \Delta\Gamma/2$. Here n is the number of steps in the histogram and $\Delta\Gamma[=(\Gamma_{max}-\Gamma_{min})/n]$ is the width of each step. Values for Γ_{min}, Γ_{max}, and n are determined relative to the average strength of $G(\Gamma_j)$. The histogram method is essentially a nonlinear least-squares technique that minimizes the sum of squared errors χ^2 with respect to each $G(\Gamma_j)$, simultaneously, such that

$$\frac{\partial}{\partial G(\Gamma_j)}\chi^2 = \frac{\partial}{\partial G(\Gamma_j)}\sum \frac{1}{\sigma_I^2}[Y_m(I\Delta\tau) - Y(I\Delta\tau)]^2 = 0 \quad (12)$$

where σ_I is the uncertainty of $Y_m(I\Delta\tau)$, with subscript m denoting the measured value.

RESULTS AND DISCUSSION

Characterization of microemulsions

The dispersed phase of the O/W microemulsions polymerized in this study consists of charged droplets. In order to measure the hydrodynamic size of the droplets based on theories of spherical particle solutions using p.c.s., it is necessary to establish a dilution scheme resulting in different volume fractions of droplets of constant radii. Since pentanol is mainly soluble in styrene, one expects the core of the droplets to contain a certain mixture of styrene and pentanol. If the ratio of this styrene–pentanol mixture to SDS remains constant, the droplets will have a constant size.

We used a dilution procedure similar to the one described by Graciaa *et al.*[9]. In our case, water containing SDS at its *cmc* was added to the microemulsion until it turned cloudy and then this mixture was titrated with a known pentanol–styrene mixture until it became transparent again. This procedure was repeated several times and for various pentanol–styrene mixtures. The generated plots for volume of pentanol–styrene mixtures *versus* volume of water are shown in *Figure 2*. The compositions of the continuous and dispersed phases

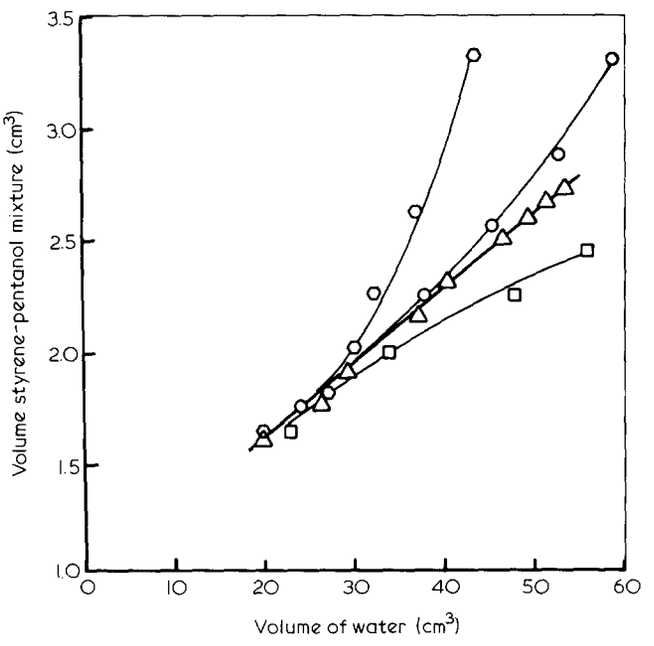

Figure 2 Plots of volume of styrene–pentanol mixtures *versus* volume of added water containing cmc in the dilution of the O/W50III. Different symbols correspond to different pentanol-to-styrene ratios such as □, △, ○, ⬡ denote styrene/pentanol = 0, 0.057, 0.1, 0.2 by volume respectively

Table 2 Compositions of the continuous and dispersed phases

Continuous phase (wt.%)		Dispersed phase (wt.%)	
H_2O	96.48	Styrene	33.57
Styrene	0.16	Pentanol	16.78
Pentanol	3.17	SDS	49.65
SDS	0.19		

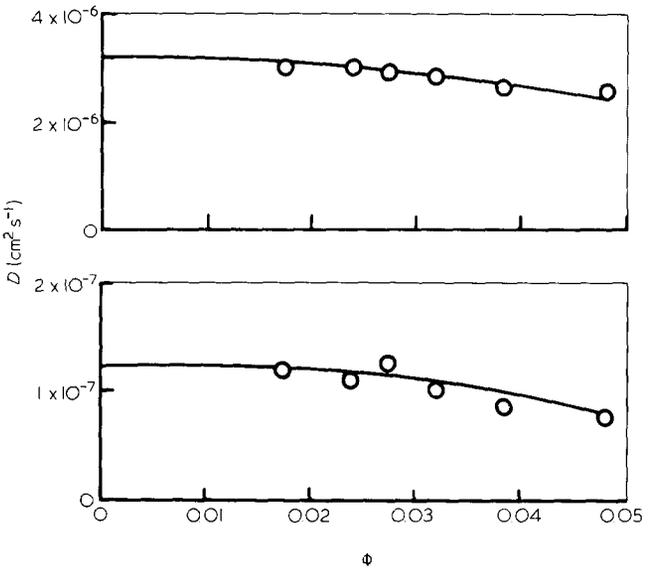

Figure 3 Plots diffusion coefficients *versus* volume fraction. $D_0 = 3.1 \times 10^{-6}$ cm^2 s^{-1} corresponds to $r_h = 0.79$ nm and $D_0 = 1.2 \times 10^{-7}$ cm^2 s^{-1} corresponds to $r_h = 20.4$ nm

computed based on the linear behaviour (triangles in *Figure 2*) in the dilution scheme are listed in *Table 2*.

The autocorrelation functions measured at different volume fractions of droplets exhibited double-exponential behaviour yielding two limiting values of diffusion coefficients when extrapolated to infinite dilution. The two diffusion coefficients were obtained from the analysis of the data as follows: The sample time on the correlator was set such that $\sqrt{A\beta|g^{(1)}(64\times\Delta\tau)|}$ was about e^{-2}. Then an unweighted, non-linear, least squares fit corresponding to the sum of two exponentials were made to 64 data points. As long as the characteristic times of the two exponentials differed by an order of magnitude, the fitting procedure converged and yielded consistent results. Plots of D *versus* volume fraction, ϕ, are shown in *Figure 3*. The faster diffusion corresponded to $D = (3.1 \pm 0.1) \times 10^{-6}$ cm^2 s^{-1} at infinite dilution and for the slower process $D = (1.2 \pm 0.1) \times 10^{-7}$ cm^2 s^{-1}. The presence of both microemulsion droplets and micelles could be the reason why correlation functions are the sum of two exponentials. If we take $D = 1.2 \times 10^{-7}$ cm^2 s^{-1} to be an apparent diffusion coefficient of the droplets, it implies an apparent hydrodynamic radius of 20.4 nm. Then at $\phi = 0.0175$, the concentration of the droplets $N = 2.65 \times 10^{14}$ droplets/cm^3 with a centre-to-centre separation of 7.5 radii. In this system there is excess SDS. If we assume the droplets contain styrene and pentanol and use a = 65 Å^2/SDS molecule, which is reported for SDS micelles in water[10], we can estimate the amount of SDS necessary to stabilize and cover the surface of the droplets. Then excess SDS can be calculated from the

total amount of SDS which yields a concentration of 0.039 mol l^{-1}. Rohde and Sackmann[11] have measured the apparent diffusion coefficient of SDS micelles in water and in NaCl solutions as a function of SDS concentration and have analysed their results by taking into account the influence of the Coulomb interaction between micelles and counterions. At $C=0.04$ mol l^{-1}, they predict $D=3\times10^{-6}$ cm^2 s^{-1} for SDS micelles in water which is in excellent agreement with $D=3.1\times10^{-6}$ cm^2 s^{-1} of this study. In the presence of excess counterions screening the charge interactions, the diffusion coefficient of SDS micelles is 0.96×10^{-6} cm^2 s^{-1} corresponding to a true hydrodynamic radius of 2.5 nm[12]. Although our value of $D=3.1\times10^{-6}$ cm^2 s^{-1} is higher by a factor of three, it can be qualitatively explained by charge interactions. It must also be pointed out that in double-exponential analysis, determination of the faster decay has higher uncertainty. Thus, we believe that $D=3.1\times10^{-6}$ cm^2 s^{-1} is due to micelles and $D=1.2\times10^{-7}$ cm^2 s^{-1} is due to microemulsion droplets.

Characterization of microemulsion polymerized styrene

For the light scattering studies, polystyrene samples prepared by microemulsion polymerization in three O/W microemulsions were dissolved in cyclohexane. Cyclohexane at 35°C is a theta solvent so that in the dilute regime, concentration dependence of the diffusion coefficient can be neglected[13]. Correlation function profiles measured at $C=0.146$ mg/ml for O/W 50I, at $C=0.366$ mg/ml for O/W 50II and at $C=0.455$ mg/ml for O/W 50III were analysed by the cumulants method and the histogram method. The results are summarized in *Table 3*. Estimated errors in *Table 3* represent uncertainties in computing the parameters from correlation functions measured at various delay times. Errors assigned in cumulants analyses also include variations due to the truncation of the cumulants expansion, equation (5), after four or five terms. For the fraction with $\bar{r}_{hL}=72$ nm based on $D_0=1.3\times10^{-4}M^{-1/2}$ from ref. 11, the limiting concentration for the dilute solution range was estimated as $M/[N_A(2r_g)^3]$ yielding 1.6 mg/ml. All the measurements were made at concentrations below this limiting value. As expected, the agreement between the two methods in predicting a mean decay rate, $\bar{\Gamma}$, was very good. The value of $\mu_2/\bar{\Gamma}^2$ obtained by the cumulants methods indicated polydisperse samples. However, the bimodal nature and the details of the decay rate distributions, which are shown in *Figure 4*, could be determined by the histogram method.

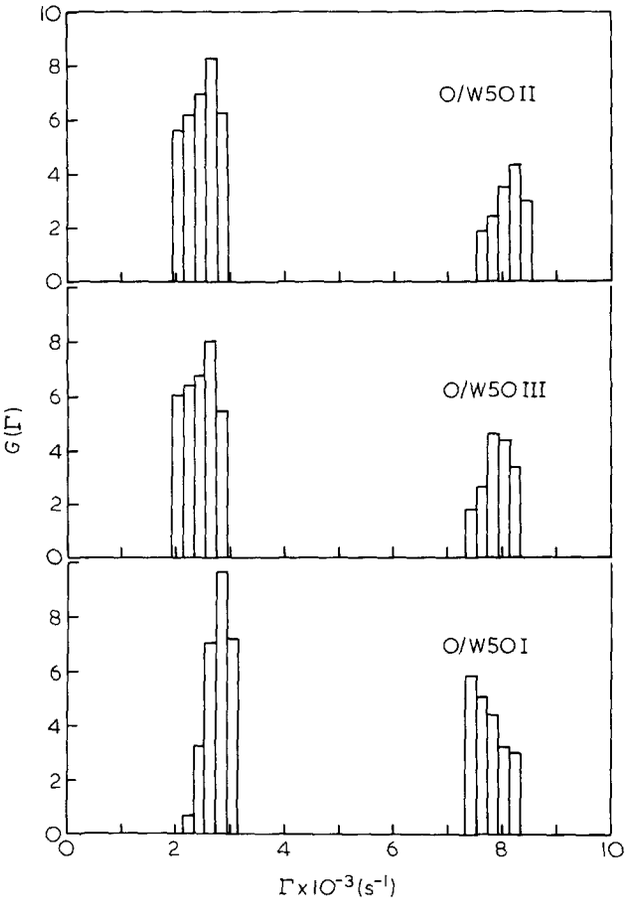

Figure 4 Plots of the linewidth distributions obtained from histogram analyses. The three polystyrene samples were dissolved in cyclohexane. The measurements were made at 35°C for $\theta=90°$

From time-averaged intensity measurements at 14 different scattering angles ($\theta=44°$ to 104°) and at five concentrations in the dilute regime, the radii of gyration were determined employing equation (2) and are listed in *Table 4*. Depending on the quality of the solvent r_h/r_g varies from 0.5 to 0.7[14]. In our case, the ratios of $\bar{r}_h$ (*Table 3*) to $\langle r_g^2\rangle_z^{1/2}$ (*Table 4*) for the three samples were 0.37, 0.36 and 0.36 respectively. Such a comparison becomes meaningless for a bimodal distribution because large and small fractions must be compared separately.

Knowledge of the ratio of areas of the large and small fractions, A_L/A_S, from the histogram analysis makes the following comparison possible. If we take the small fraction to be composed of random coils with $r_h/r_g=0.6$, then r_{gS} can be determined from r_{hS}. At $\theta=90°$, assuming

Table 3 Parameters computed by the histogram and cumulants methods

	O/W 50 I C = 0.146 mg/ml		O/W 50 II C = 0.366 mg/ml		O/W 50 III C = 0.445 mg/ml	
Parameters	Histogram	Cumulants	Histogram	Cumulants	Histogram	Cumulants
$\bar{\Gamma}$ (s^{-1})	4987 ± 50	5137 ± 124	4209 ± 50	4497 ± 84	4323 ± 110	4642 ± 170
$\bar{D}\times10^8$ (cm^2 s^{-1})	8.24 ± 0.10	8.49 ± 0.21	6.96 ± 0.10	7.43 ± 0.13	7.15 ± 0.20	7.67 ± 0.28
$\bar{r}_h$ (nm)	35.7 ± 0.03	34.7 ± 0.8	42.3 ± 0.6	39.7 ± 0.7	41.2 ± 1.2	38.5 ± 1.4
$\mu_2/\bar{\Gamma}^2$	0.25 ± 0.10	0.39 ± 0.13	0.39 ± 0.10	0.70 ± 0.16	0.36 ± 0.10	0.75 ± 0.20
$\bar{\Gamma}_{hL}$ (s^{-1})	2786 ± 50	–	2468 ± 100	–	2456 ± 50	–
$\bar{r}_{hL}$ (nm)	63.9 ± 1.5	–	72.2 ± 4.0	–	72.5 ± 4.0	–
$\bar{\Gamma}_S$ (s^{-1})	7782 ± 50	–	8090 ± 50	–	7920 ± 80	–
$\bar{r}_{hS}$ (nm)	22.9 ± 0.2	–	22.0 ± 0.3	–	22.5 ± 0.3	–
A_L/A_S	1.27 ± 0.05	–	2.23 ± 0.10	–	1.92 ± 0.5	–

the ratio of the intensities of the two fractions is proportional to the ratio of areas in $G(\Gamma)$, the contribution of the small fraction can be estimated and subtracted from the total measured intensity to obtain the contribution of the large fraction at each scattering angle. Then from a plot of $(HC/R_v^*)_L$ *versus* $\sin^2(\theta/2)$, r_{gL} could be computed to obtain an $(r_h/r_g)_L$ value that can be compared to the assumed value of 0.6 for the small fraction. The resolution of the total intensity into the contribution of the two fractions is illustrated in *Figure 5* for O/W 50III and the results for the three samples are summarized in *Table 5*. The molecular weights of the two fractions were calculated from hydrodynamic radii based on the relation in ref. 13.

In emulsion polymerization, initiation by a water-soluble free-radical initiator starts in the aqueous phase[15]. Either radicals penetrate the monomer-swollen micelles and polymerize the solubilized monomer or, radicals initiate the dissolved monomer molecules, forming oligomeric radicals that further grow into latex particles. Droplets that contain most of the monomer act as reservoirs and supply monomer by diffusion for growth of particles formed by either of the two mechanisms. Droplets do not compete in capturing radicals because the surface area of the droplets is smaller than that of micelles.

In principle, if the droplets can be made much smaller, resulting in much larger surface area, both mechanisms of initiation could contribute. Using mixtures of sodium hexadecyl sulphate and hexadecanol as emulsifier to produce drops of 0.5–1 μm, in comparison to ~5 μm drops with only surfactant as emulsifier, Ugelstad *et al.*[16] have initiated styrene droplets. They report bimodal electron micrographs of latex particles indicating a second mechanism involving initiation and polymerization in droplets. In a more recent study, Piirma and Chang[17] have found that the conversion–time curves, in the emulsion polymerization of styrene, show two rate regions. The second-stage occurs at ~40% conversion and exhibits a faster rate and consequently produces a bimodally dispersed latex.

In ref. 17, the measured radii of the two fractions by electron microscopy are 60 nm, and 210 nm at 92.5% conversion with the ratio of large to small radii being 3.5. We measured hydrodynamic radii of 22 nm and ~70 nm with $\bar{r}_{hL}/\bar{r}_{hS} = 3.2$. A possible explanation for the lower radii measured in this study is that the droplets are smaller and in the presence of pentanol, chain transfer and termination reactions might produce a lower molecular weight polymer. However, the ratio of the two sizes are similar which indicates similar conditions for the rates of particle growth.

In our case, the solubility of styrene in the continuous phase is very low; practically all of the monomer is in the droplets. The droplets are negatively charged and the penetration of the radicals into the droplets is hindered. Furthermore, the presence of pentanol, which can act as a chain-transfer agent, complicates the growth kinetics. Although the bimodality of the polymer product is not unusual and indicates the existence of two mechanisms of particle nucleation and growth, further studies are necessary in order to understand the details. One expects variations due to minimization of charge effects in the presence of counterions or if the initiator were oil soluble instead of water soluble. These effects are being studied and will be reported in a subsequent communication.

Table 4 The radii of gyration from time-averaged intensity measurements

Sample	$\langle r_g^2 \rangle_z^{1/2}$ (nm)
O/W 50 I	95.0 ± 10
O/W 50 II	118 ± 10
O/W 50 III	115 ± 10

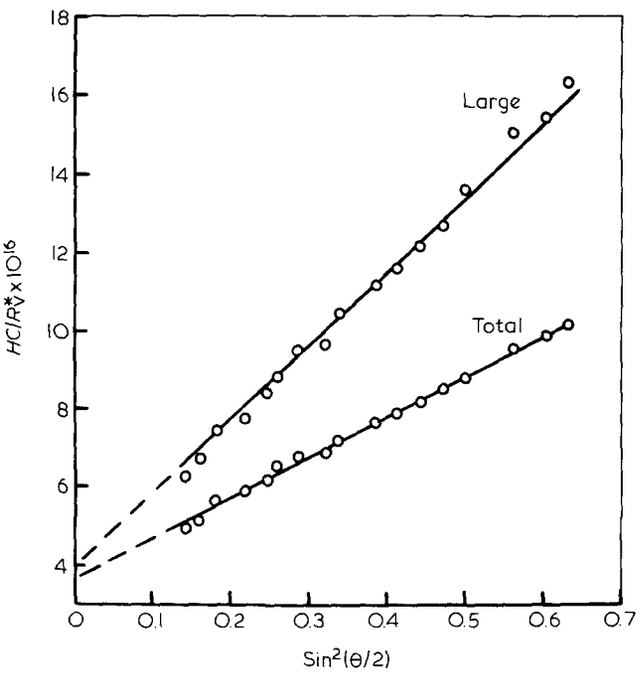

Figure 5 Plots of HC/R_v^* *versus* $\sin^2(\theta/2)$ for the polystyrene sample isolated from O/W50III at C=0.455 mg/ml. The line labelled 'total' represents the measured values. HC/R_v^* for the large fraction was obtained by subtracting the intensity of the small fraction and yields r_{gL}=128 nm

Table 5 Hydrodynamic radii, radii of gyration and molecular weights of the large and small fractions

	O/W 50 I	O/W 50 II	O/W 50 III
$\bar{r}_{hS}$ (nm)	22.9	22.0	22.5
$\bar{r}_{gS}$ (nm)	38.2	36.7	37.5
$\bar{r}_{hS}/\bar{r}_{gS}$	0.6	0.6	0.6
M_S (g mol^{-1})	1.02 x 10^6	0.94 x 10^6	0.97 x 10^6
$\bar{r}_{hL}$ (nm)	63.9	72.2	72.5
$\bar{r}_{gL}$ (nm)	119 ± 10	145 ± 12	128 ± 10
$\bar{r}_{hL}/\bar{r}_{gL}$	0.53 ± 0.05	0.49 ± 0.05	0.57 ± 0.05
M_L (g mol^{-1})	7.97 x 10^6	10.1 x 10^6	10.3 x 10^6

CONCLUSIONS

Polymerization of styrene in O/W microemulsions, where styrene was in the dispersed phase and the initiator, potassium persulphate, was soluble in the continuous phase, produced polystyrene containing two fractions of different molecular weights. After establishing an appropriate dilution scheme for the initial microemulsions, droplets of 40.8 nm diameter were measured at infinite dilution using p.c.s. The isolated polymer products were characterized by combining p.c.s. and time-averaged intensity measurements. Bimodality of the size distri-

bution of the products were determined by the histogram method. The information on the hydrodynamic radii and the details of the size distribution obtained from p.c.s. were used to resolve the intensity data into contributions of each fraction, thus yielding the molecular weight and radius of gyration of the two fractions. The sizes of the two fractions differed by a factor of 3.2 resulting in an order of magnitude difference in molecular weights.

Our results indicate that in a microemulsion smaller droplets presenting an increased surface area can compete with micelles in the capture of radicals. The bimodal nature of the products provide evidence for two mechanisms of initiation and particle growth.

ACKNOWLEDGEMENTS

This work was partially supported by National Science Foundation, Grant No. CPE-80-21952. As a recipient of a fellowship, P. L. Johnson gratefully acknowledges American Association of University Women Education Foundation.

REFERENCES

1 Shinoda, K. S. and Friberg, S. *Adv. Colloid. Interface Sci.* **4**, 281 (1975)
2 Stoffer, J. O. and Bone, T. *J. Dispersion Sci. Technol* 1980, **1**,
3 Stoffer, J. O. and Bone, T. *J. Polym. Sci., Polym. Chem. Edn.* 1980, **18**, 2641
4 Leong, Y. S. and Candu, F. *J. Phys. Chem.* 1982, **86**, 2269
5 Gulari, Es. and Chu, B. *Bioplomers* 1979, **18**, 2943
6 Yamakawa, H. 'Modern Theory of Polymer Solution', Harper & Row, New York (1971)
7 Koppel, D. E. *J. Chem. Phys.* 1972, **57**, 4814
8 Gulari, Es., Gulari, Er., Tsunashima, Y. and Chu, B. J. *Chem. Phys.* 1979, **70**, 3965
9 Graciaa, A., Lachaise, J., Martinez, A., Bourrel, M. and Chambu, C. *C. R. Acad. Sci.* 1976, **282B**, 547
10 Cazabat, A. M. and Langevin, D. *J. Chem. Phys.* 1981, **74**, 3148
11 Rohde, A. and Sackmann, E. *J. Colloid and Inteface. Sci.* 1979, **70**, 494
12 Corti, M. and Degiorgio, V. *Chem. Phys. Lett.* 1978, **53**, 237
13 Gulari, Er., Gulari, Es., Tsunashima, Y. and Chu, B. *Polymer* 1979, **20**, 347
14 Nose, T. and Chu, B. *Macromolecules* 1979, **12**, 1122
15 Fitch, R. M. in Polymer Colloids (Ed R. M. Fitch), Plenum Press, New York, 1971
16 Ugelstad, J., Hansen, F. K. and Lange, S. *Makromol. Chem.* 1974, **175**, 507
17 Piirma, I. and Chang, M. *J. Polym. Sci: Polym. Chem. Edn.* 1982, **20**, 489